Electronic structure of $PrBa_2Cu_3O_7$ from LAPW band structure calculations

1994 J. Phys.: Condens. Matter 6 2347

(http://iopscience.iop.org/0953-8984/6/12/008)

J. Phys.: Condens. Matter 6 (1994) 2347–2356. Printed in the UK

Electronic structure of $PrBa_2Cu_3O_7$ from LAPW band structure calculations

Claudia Ambrosch-Draxl†, Peter Blaha‡ and Karlheinz Schwarz‡

† Institut für Theoretische Physik, Universität Graz, A-8010 Graz, Universitätsplatz 5, Austria
‡ Institut für Technische Elektrochemie, Technische Universität Wien, A-1060 Vienna, *Getreidemarkt 9/158, Austria*

Received 22 October 1993

Abstract. We have performed band structure calculations for $PrBa_2Cu_3O_7$ using the full-potential LAPW method, which is based on density functional theory. The Pr 4f electrons are treated as valence states and form narrow bands at the Fermi level. Furthermore we have simulated a Pr valency of 3+ (4+) by treating the Pr 4f states as localized states with a fixed occupation of 2 (1). We have determined partial charges, densities of states, difference densities, electric field gradients, and their asymmetry parameters for this system and discuss the differences between the 'itinerant case' and the two model calculations representing the localized f states. The corresponding total energies yield the results that the itinerant f states are the most stable, followed by Pr with a 3+ valency, and the 4+ being the least stable. The overall electronic structure obtained by the itinerant calculation is rather close to the trivalent Pr case.

1. Introduction

In the high-temperature superconductor $YBa_2Cu_3O_7$ (YBCO) the substitution of yttrium by rare earth elements has in most cases hardly any effect on the critical temperature. The corresponding phase with Ce and Tb could not be synthesized, but Pr is a real exception, since its presence destroys superconductivity. In $Y_{1-x}Pr_xBa_2Cu_3O_7$ the critical temperature T_c monotonically decreases with the Pr concentration x from $T_c = 92$ K to $T_c = 0$ K for $x = 0.55$. The completely substituted $PrBa_2Cu_3O_7$ (PBCO) is an antiferromagnetic insulator with magnetic moments on Pr as well as on Cu(2) in the copper–oxygen plane.

Several possible mechanisms for the suppression of superconductivity are discussed in the literature [1]. One of them is related to the valency of the Pr atom, which can be tri- or tetravalent. When the trivalent Y is replaced by a tetravalent Pr, the additional electron can fill up part of the holes in the copper–oxygen plane, which are responsible for superconductivity in YBCO. Another reason for the disappearance of superconductivity could be the observed antiferromagnetic moment at the Pr site, but since the replacement of Y by other magnetic rare earth atoms does not affect superconductivity this is not likely to be the reason for this effect. The suggestion has been made that a strong hybridization between Pr 4f states and conduction bands could destroy superconductivity [2]. Many experiments have been performed in order to investigate this problem, but until now the valency of Pr is still not completely clear, although there is evidence for a trivalent Pr by many spectroscopies. An extensive discussion on the experimental situation of PBCO is given by Hilscher *et al* [3].

0953-8984/94/122347+10$19.50

The main question is, whether the Pr 4f states hybridize with O 2p states forming bands near the Fermi energy, or whether the Pr 4f states are localized with an integer Pr valency of +3 or +4. In order to investigate this problem we present an analysis of the electronic structure of PBCO in terms of partial charges, densities of states (DOS), difference densities, electric field gradients, and their asymmetry parameters. Since band structure calculations are known to favour 'itinerant' band states (hybridization) over localized states, we simulate an integer valency of Pr (3+ as well as 4+) by treating the Pr 4f states as localized core states with a fixed occupation number.

The first results from our preliminary calculations have been published elsewhere [4]. Now we present data which are better converged due to higher LM components in the non-spherical part of the potential. The general picture we obtain from our calculations is in good agreement with LMTO–ASA calculations by Guo and Temmerman [5], although they did not consider the antiferromagnetic ordering of the Pr sublattice.

Recently, a model for the electronic structure of PBCO was proposed [6] based on insulating CuO_2 planes, mixed-valent Pr ions and Cu–O chains described with a t–J model. The absence of superconductivity is explained by hybridized states of Pr 4f and O $2p_\pi$ orbitals which bind doped holes to Pr sites.

2. Crystal structure

$Y_{1-x}Pr_xBa_2Cu_3O_7$ has an orthorhombic lattice with space group *Pmmm* for the entire range from $x = 0$ to $x = 1$. The crystal data were taken from Neumeier *et al* [7], who determined the lattice parameters by neutron diffraction, increasing the Pr content up to $x = 1$.

In this paper the same labelling of the atoms is used as in YBCO, namely: Cu(1) and O(1) are the chain atoms, Cu(2), O(2), and O(3) form the copper–oxygen-planes, and O(4) are the bridging (apical) oxygen atoms between the chains and the planes.

Taking into account the antiferromagnetic ordering of the Pr atoms in all three directions the unit-cell volume is doubled and can be described by the space group *Fmmm*. There exist two Pr atoms (Pr(1) and Pr(2)), which are chemically equivalent, but differ in their magnetic behaviour ('spin-up' of Pr(1) is equivalent to 'spin-down' of Pr(2) and vice versa). Due to the space group the same is true for Ba.

Antiferromagnetic ordering of the Cu(2) atoms would cause either the loss of inversion symmetry or a further doubling of the unit cell; thus for computational reasons we ignore in our present calculations the magnetic ordering in the Cu(2) sublattice.

3. Models

The *itinerant* calculation was carried out by a standard full-potential spin-polarized band calculation, including the Pr 4f electrons as band states which hybridize with all other valence states. In order to simulate localized 4f states we switch off this hybridization and treat the Pr 4f states in the spherical part of the potential as atomic-like core states. The two relevant cases are denoted as '3+' or 'PBCO3+' and '4+' or 'PBCO4+' and are characterized by the integer occupation number of 2 and 1 for the 4f states.

Furthermore, we tried another model calculation, in which we treated the 4f states in an additional (full-potential) band calculation as semi-core states, in order to allow the Pr 4f charge density to be of non-spherical symmetry. These calculations, however, turned out to be extremely difficult to converge and thus such results are not described here.

4. Computational details

The calculations were performed via the full-potential LAPW method using the optimized version WIEN93 of the originally published WIEN code [8]. Atomic sphere radii of 2.83, 2.9, 1.9 and 1.55 au were taken for Pr, Ba, Cu and O, respectively. We used about 1850 plane wave basis functions, and a maximum of $l = 12$ in the expansion of the radial wave functions. Inside the spheres the potential and the charge density were expanded into crystal harmonics up to $L = 6$ for Pr, $L = 4$ for Ba, Cu, O(1), and O(4); only for O(2) and O(3) was the expansion limited to $L = 3$; in the interstitial region a Fourier series with 2025 $\boldsymbol{K}$ stars was used. For the Brillouin zone (BZ) integrations a tetrahedron method with 18 special k points was used. The Cu 3p states (lying at about -4.5 Ryd) were treated as semi-core states in an additional band calculation using five special k points.

5. Results

5.1. Densities of states

The total densities of states for PBCO, PBCO3+ and PBCO4+ are compared in figure 1 and the main contributions are labelled: the valence bands (between -7 and $+2$ eV) are dominated by O 2p and Cu 3d orbitals, the bands around -10.5 eV originate from the Ba 5p states and the O 2s bands lie at about -17 eV.

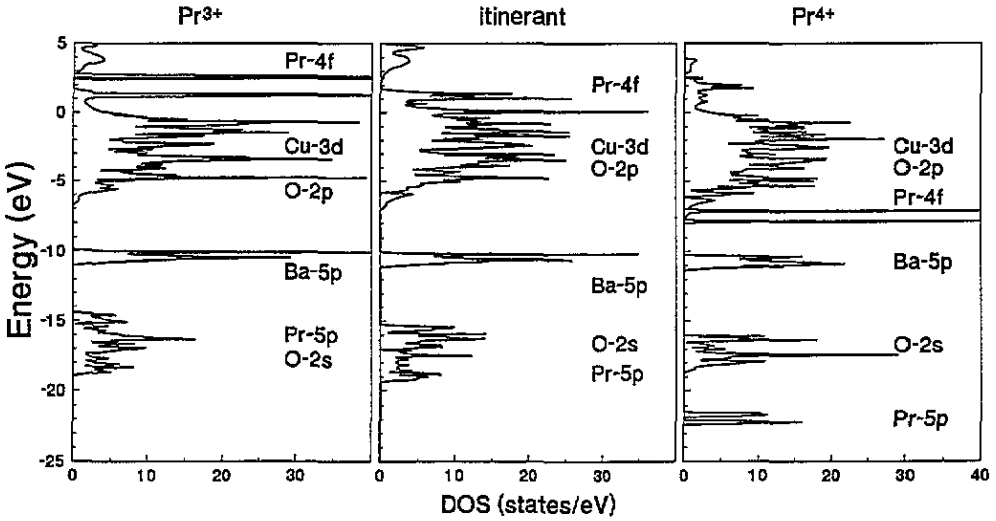

Figure 1. The total densities of states (including both spin directions) in states per eV and formula unit for the three models.

In the itinerant case the Pr 4f states form two narrow bands split by about 1 eV. The Fermi level falls into the lower f bands which are partly occupied for spin-up, but are almost unoccupied for spin-down at the Pr(1) position (and vice versa for Pr(2)), leading to an antiferromagnetic moment of 1.5 μ_B in the Pr sublattice.

In the model calculations representing the tri- and tetravalent Pr, the 4f states are treated as core-like states (with the integer occupation numbers 2 and 1, respectively) omitting the

hybridization with other bands. The energies of these atomic-like 4f states are artificially added in figure 1 to the DOS for Pr^{3+} and Pr^{4+}, in order to illustrate their energetic positions relative to the other bands. In the 3+ (4+) case the split f bands are at about +1.2 and +2.6 eV (−7.1 and −8.0 eV). Thus in PBCO3+ the 4f states lie above, while in PBCO4+ they are far below E_F.

The Pr charge affects the positions of all lower lying Pr core levels; e.g. the Pr 5p states lie around −18 eV in the 3+ case, while these levels are about 6 eV lower in the 4+ case. Similar shifts are found for all other Pr core levels and even for the unoccupied Pr 5d states, a trend already reported by Guo and Temmerman [5]. Based on their calculations Kircher *et al* [9] interpreted the optical response of PBCO obtained by ellipsometric measurements. They did not observe peaks in the optical spectrum, which should arise from transitions into the unoccupied Pr 5d levels in a tetravalent Pr compound, so they concluded that their results could be explained under the assumption of trivalent Pr ions.

Besides the Pr 4f states (which are treated in an atomic model and are occupied with two electrons, although they clearly lie above the Fermi level) the general features of the DOS of itinerant PBCO are very similar to those of PBCO3+, indicating that the band picture gives a Pr valency close to 3+. We find that the lower-lying Pr states (e.g. Pr 5p) are affected much more by the difference in the 4f occupation numbers than oxygen, barium, and copper states, and thus spectroscopy of the latter is not really the tool to investigate the valency of Pr.

5.2. Charge distribution

In the LAPW formalism a symmetry decomposition of the electronic charge inside the spheres can be made according to l and m. Note that often a large fraction of the charge lies outside the atomic sphere and the partial charges depend on the choice of sphere radii. In table 1 the partial charges for the valence states of Pr (5s, 5p, 5d, 4f), Ba (5s, 5p, 5d), Cu (4s, 4p, 3d), and O (2s, 2p, 3d) are shown. The values represent only one spin direction. For the non-magnetic copper (as assumed in our present calculation) and oxygen atoms the partial charges are the same for both spins. For Pr and Ba, however, the antiferromagnetic ordering has to be taken into account: the spin-up charges of Pr(1) (Ba(1)) are equal to the spin-down charges of Pr(2) (Ba(2)) and vice versa. The Pr atoms show a strong spin polarization, mainly in the f-like partial charge resulting in an antiferromagnetic moment of 1.5 μ_B (see also table 3). The d-like charge distribution among the five Pr 5d orbitals is very similar to that of the Y 4d orbitals in YBCO [10]. The magnetic moment of Pr does not affect the Ba sites, for which negligible differences between the partial charges of the two spin directions are found. The Pr substitution hardly affects the Cu(1) position, for which we find almost the same partial charges as in YBCO. In order to gain more insight into how the copper–oxygen plane is affected by Pr substitution, we show in table 2 a direct comparison of the Cu(2) and O(3) charges of the three PBCO models with YBCO. We note as the main conclusion that both the Cu(2) d and O(3) p charges are affected by only a few hundredths of an electron (independent of the model used). At the Cu(2) site differences between YBCO and PBCO are found in the asymmetry of the Cu d charge, which is smaller in PBCO. (The ratio of $d(x^2-y^2)/d(z^2)$ charges is 0.87 in PBCO but 0.82 in YBCO.) The anisotropy of the d-like charges also depends on the Pr valency, as can be seen in table 2. The occupation number of Cu(2) $d(x^2-y^2)$ is smallest for the 3+ case and largest for 4+, while for $d(z^2)$ and $d(xy)$ it is the other way around. This fact leads to a larger asymmetry among the d-like charges for the 3+ than for the 4+ case. Ongoing from YBCO to PBCO the partial charges of the plane oxygen atoms, O(2) and O(3), are also redistributed. Although the changes in the partial charges are rather small, these differences between YBCO and PBCO lead to a reduced

anisotropy of the corresponding oxygen p-like charges in PBCO (itinerant case). Among the three cases (3+, itinerant, 4+) the oxygen anisotropy is largest for the 3+ case (table 2). Ongoing from 3+ to 4+ the increasing occupation numbers of Cu(2) $d(x^2 - y^2)$, O(2) p_x and O(3) p_y partial charges could be interpreted as hole filling. We, however, believe that we can rule out a tetravalent Pr, since the total p- and d-like charges of the plane atoms are not significantly affected by the Pr substitution, so that in comparison with YBCO there is almost no filling of the holes in the copper–oxygen planes, but a charge redistribution among the different symmetries. This fact is consistent with the EELS measurements of Fink *et al* [11].

Table 1. Site projected partial charges (in electrons) of the valence states and their symmetry decomposition of the p- and d-like charges, where the cartesian coordinates are assumed to be parallel to the crystallographic axes. The values represent only one spin direction. Due to antiferromagnetic ordering the partial charges for Pr(1) spin-up are identical to Pr(2) spin-down and vice versa. The same is true for Ba. For comparison see the partial charges of YBCO (table 2 of [10]).

	s	p	d	f	p_x	p_y	p_z	d_{z^2}	$d_{x^2-y^2}$	d_{xy}	d_{xz}	d_{yz}
Pr(1)	1.019	2.940	0.402	1.829	0.977	0.980	0.982	0.043	0.103	0.038	0.106	0.111
Pr(2)	1.019	2.935	0.384	0.350	0.976	0.978	0.981	0.041	0.099	0.036	0.102	0.106
Ba(1)	0.991	2.781	0.141	0.035	0.932	0.927	0.923	0.030	0.018	0.045	0.030	0.017
Ba(2)	0.991	2.781	0.140	0.035	0.932	0.927	0.923	0.029	0.018	0.045	0.030	0.017
Cu(1)	0.115	0.100	4.317	0.010	0.015	0.034	0.051	0.716	0.831	0.918	0.921	0.930
Cu(2)	0.096	0.086	4.357	0.007	0.034	0.034	0.018	0.871	0.759	0.916	0.904	0.907
O(1)	0.773	1.664	0.003		0.586	0.451	0.626					
O(2)	0.772	1.690	0.005		0.512	0.595	0.583					
O(3)	0.772	1.686	0.005		0.595	0.508	0.583					
O(4)	0.771	1.681	0.004		0.587	0.601	0.493					

Table 2. Partial charges (in electrons) of the Cu(2) and O(3) valence states and their symmetry decomposition of the p- and d-like charges for the cases 3+, itinerant, and 4+ compared with YBCO (taken from [10]). The values represent only one spin direction.

		p	d	p_x	p_y	p_z	d_{z^2}	$d_{x^2-y^2}$	d_{xy}	d_{xz}	d_{yz}
	3+	0.086	4.343	0.035	0.034	0.017	0.875	0.728	0.924	0.905	0.911
Cu(2)	itinerant	0.086	4.357	0.034	0.034	0.018	0.871	0.759	0.916	0.904	0.907
	4+	0.086	4.371	0.034	0.034	0.018	0.867	0.776	0.915	0.906	0.907
	YBCO	0.091	4.343	0.038	0.035	0.018	0.879	0.719	0.926	0.910	0.909
	3+	1.699		0.615	0.489	0.595					
O(3)	itinerant	1.686		0.595	0.508	0.583					
	4+	1.697		0.595	0.520	0.582					
	YBCO	1.683		0.601	0.497	0.585					

In the 'localized' cases the 4f occupation is constrained to integer values, causing the corresponding magnetic moments of $2\mu_B$ for 3+, and $1\mu_B$ for 4+ (table 3), while for the itinerant case the magnetic moment is $1.5\mu_B$ determined self-consistently. Note that about 0.1 4f electrons for both spin directions are still present in PBCO3+ and PBCO4+, which represent the partial wave expansion of tails from wavefunctions coming from neighbouring atoms. The total charge Q inside the Pr atomic sphere is the same for the itinerant and

Table 3. The total charge Q, the 4f charge q^{4f} (decomposed into spin-up and spin-down) and the magnetic moment M corresponding to the atomic sphere of Pr in the three models.

	3+	itinerant	4+
Q	56.9e	56.9e	56.5e
q^{4f} ↑	2.1e	1.8e	1.1e
↓	0.1e	0.3e	0.1e
M	2.0μ_B	1.5μ_B	1.0μ_B

the 3+ case. The total charge for the 4+ case is only 0.4 electrons smaller than for 3+, although the occupation number of 4f electrons differs by 1. This means that the extra charge of the missing f electron is partly screened by other electrons.

5.3. Electron densities

The charge distribution of PBCO is shown as the difference density $\Delta\rho$ in the (100) plane (figure 2), where $\Delta\rho$ is the difference between the crystalline density and the superposed ionic densities of the free ions Pr^{3+}, Ba^{2+}, Cu^{+}, and $O^{-10/7}$. The ionicity of oxygen is chosen such as to keep charge neutrality of the completely ionic reference system. negative contour lines indicate that the charge density in the crystal is smaller than in the corresponding ion and that the antibonding Cu–O orbitals are not fully occupied. The overall difference to the corresponding $\Delta\rho$ in YBCO (see figure 3 of [10]) is very small, especially along the Cu–O chains. The largest effect is found in the Cu–O planes (see also table 2), where in YBCO $\Delta\rho$ has positive regions near O(3), which are essentially lost in PBCO (figure 2) indicating a small charge asymmetry directly related to a smaller electric field gradient at this position (see section 5.4). A similar but less pronounced effect occurs at Cu(2), where the asymmetry (and consequently the electric field gradient) is also smaller than in YBCO.

Figure 3 shows how the Pr valency affects the charge distribution in the copper–oxygen planes. The figure shows the difference densities between PBCO and PBCO3+ (figure 3(a)) and PBCO and PBCO4+ (figure 3(b)) as contour plots through the copper–oxygen planes. The positive part of the difference density at O(3) in the upper panel (figure 3(a)) and the corresponding negative part in figure 3(b) indicate an increase of p_y charge (corresponding to the orbital pointing from O(3) towards Cu(2) ongoing from 3+ to 4+ (see table 2). We note that for O(3) the difference between PBCO and PBCO4+ is smaller than and opposite in sign from that between PBCO and PBCO3+. For the O(3) out-of-plane component p_z PBCO has less density than PBCO3+, while there is hardly any difference between PBCO and PBCO4+. A similar analysis can be made for Cu(2), where we find a slight increase of charge in the b direction (i.e. in the $d(x^2 - y^2)$ orbital) in the itinerant case with respect to 3+, whereas for the c direction it is the other way around. However, with respect to 4+ (figure 3(b)) the gain and losses around Cu(2) are opposite to those of the 3+ case (figure 3(a)). This asymmetry of the charges strongly influences the electric field gradient, which is discussed in the next section. The effect of the different Pr charge states on the total Cu or O charges is very small. In a recent paper by Fehrenbacher and Rice [6] such covalent interactions between O and Pr are discussed, which are at least qualitatively consistent with our findings.

5.4. The electric field gradient

The electric field gradient (EFG) is defined as the second derivative of the electrostatic potential at the nucleus, written as a traceless tensor. It can be computed directly from

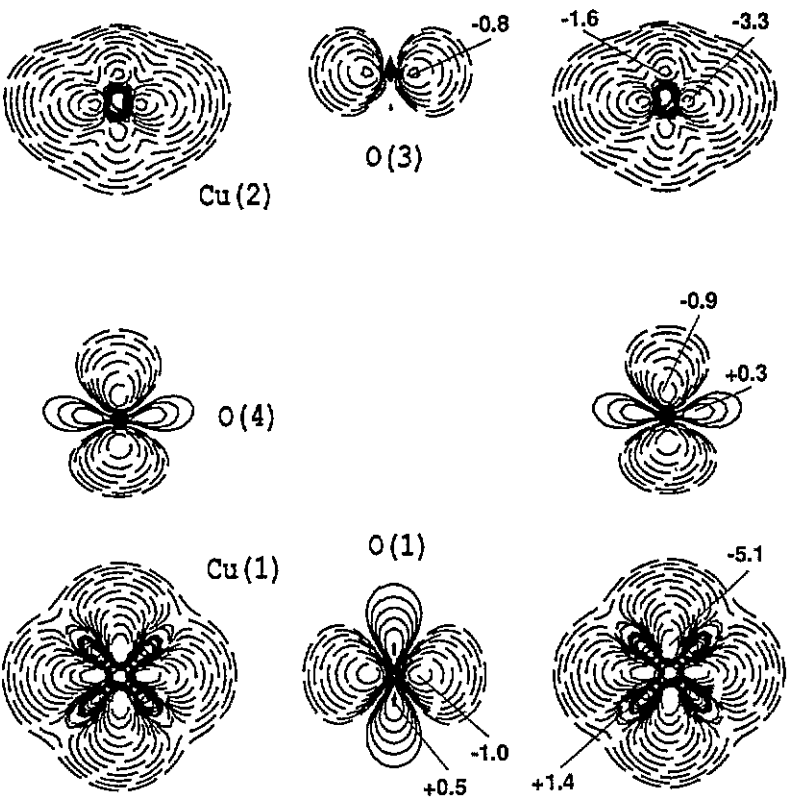

Figure 2. The difference density $\Delta\rho$ for PBCO taken between the crystalline and the superposed ionic densities of Pr^{3+}, Ba^{2+}, Cu^{+}, and $O^{-10/7}$. The contour plot shows a plane parallel to the b and c axes. Minima and maxima are labelled in units of e Å^{-3}. The contour curves start at ± 0.1 and differ by a factor of $\sqrt{2}$. Positive values are indicated by full curves, negative values by broken curves.

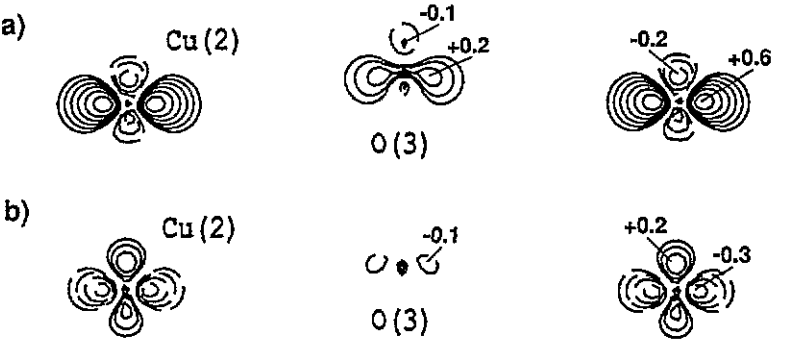

Figure 3. The difference density in the copper–oxygen plane between the valence densities of (*a*) PBCO and PBCO3+ and (*b*) between PBCO and PBCO4+. The contour plot shows a plane parallel to the b and c axes through the atoms Cu(2) and O(3) (top of figure 2) with the same normalization as in figure 2.

the charge density using a method developed by Blaha *et al* [12] which was successfully applied to various systems.

We have already performed such calculations for $YBa_2Cu_3O_{7-x}$ [10] and $YBa_2Cu_4O_8$ [13] and have shown that the EFG is very sensitive to the anisotropy of the charge distribution. (For definitions and detailed information see [10].) Our first results for PBCO have been published elsewhere [4].

Table 4. Electric field gradient components V_{xx}, V_{yy} and V_{zz} (in 10^{21}V m^{-2}), the principal component, denoted as EFG, and the asymmetry parameter η for the Ba, Cu and O positions for PBCO. The theoretical results correspond to the itinerant case and the experimental data are taken from Reyes *et al* [14].

		V_{xx}	V_{yy}	V_{zz}	EFG	η
Pr	theory	3.4	0.3	−3.7	−3.7	0.85
Ba	theory	−8.7	0.8	7.9	−8.7	0.81
Cu(1)	theory	−5.2	6.5	−1.3	6.5	0.60
	experiment				±8.2	
Cu(2)	theory	1.0	1.5	− 2.5	−2.5	0.19
	experiment				∓6.7	0.00
O(1)	theory	−5.4	17.8	−12.4	17.8	0.39
O(2)	theory	9.4	−5.7	−3.7	9.4	0.21
O(3)	theory	−5.8	9.8	−4.0	9.8	0.19
O(4)	theory	−4.6	−7.4	12.0	12.0	0.23

The EFG tensor and the corresponding asymmetry parameter η at each atomic position of PBCO are summarized in table 4. Experimental data are only available for the copper positions [14]. The theoretical EFG at Cu(1) is smaller than the experimental one by about 20%, which is a rather good agreement between theory and experiment (not as good as in YBCO). For Cu(2) the situation is comparable to YBCO, and the theoretical value is again too small by a factor of more than 2. At the oxygen positions the EFG and asymmetry parameters are very similar to those in YBCO.

The EFG at the copper sites is influenced by the Pr valency. Therefore in table 5 the tensor components and the asymmetry parameters from the model calculations for 3+ and 4+ are compared with the itinerant case. We find that not only at Cu(1) is the EFG larger for 3+, but at Cu(2) the EFG and η agree perfectly with experiment for a Pr valency of +3, whereas for the 4+ case the EFG components are very small with a large η-value. From this point of view we can rule out a tetravalent Pr.

There are also consequences for the EFG at the oxygen positions. While the effect of the Pr valency is very small at O(1) and O(4), which we have seen already in the partial charges, the EFG at O(2) and O(3) increases by about 50% ongoing from 4+ to 3+. However, for these sites the difference between 4+ and the itinerant case is rather small (about 10%), as already shown in the corresponding partial charges or difference densities (figure 3). The dependence of the oxygen EFG on the Pr valency is due to the fact that a reduction of the number of 4f electrons (ongoing from 3+ to 4+) causes a redistribution of e.g. O(3) p charge into p_y orbitals, i.e. a partial filling of the Cu O pd_σ holes (table 2).

From the present model calculations with localized f states we cannot give quantitative results for the EFG at the Pr site, because the Pr 4f states were treated in the spherically symmetric part of the potential and do not give a realistic asymmetry of the 4f charge distribution. We can estimate the 4f contribution to the EFG by using occupations according to Hund's rule. Unfortunately in this case both Pr^{3+} and Pr^{4+} would lead to the same EFG

Table 5. Electric field gradient components (in 10^{21} Vm^{-2}) and the asymmetry parameter η at the copper and oxygen positions in PBCO for the three models.

		V_{xx}	V_{yy}	V_{zz}	η
	3+	−5.9	7.0	−1.1	0.69
Cu(1)	itinerant	−5.2	6.5	−1.3	0.60
	4+	−4.8	6.1	−1.3	0.56
	3+	3.0	2.6	−5.6	0.07
Cu(2)	itinerant	1.0	1.5	−2.5	0.19
	4+	−0.4	0.6	−0.2	0.33
	3+	−6.5	17.8	−11.3	0.27
O(1)	itinerant	−5.4	17.8	−12.4	0.39
	4+	−5.7	17.2	−11.5	0.33
	3+	13.1	−8.7	−4.4	0.32
O(2)	itinerant	9.4	−5.7	−3.7	0.21
	4+	8.3	−5.1	−3.2	0.23
	3+	−8.6	13.7	−5.1	0.25
O(3)	itinerant	−5.8	9.8	−4.0	0.19
	4+	−5.2	8.3	−3.1	0.25
	3+	−5.2	−6.5	11.7	0.11
O(4)	itinerant	−4.6	−7.4	12.0	0.23
	4+	−4.4	−7.2	11.6	0.23

(since an f electron in an $m = 2$ state does not contribute to the EFG). Nevertheless we can estimate that the Pr EFG would be about 20 times larger for a localized Pr 4f state than for the itinerant f electrons. Therefore it would be very interesting to obtain experimental (NMR) data for the Pr EFG.

5.5. Total energies

If we compare the total energies for the two model calculations we find that Pr with a 3+ valency would be more stable than that with 4+, with a total energy difference of about 3 eV per formula unit. This trend has already been found by Guo and Temmerman [5]. So we again can rule out a Pr valency of +4. The total energy of the standard band calculation is of course the lowest, by about 3 eV with respect to the 3+ case. Therefore we just compare the two model calculations with each other.

6. Summary

In order to investigate the valency of Pr in PBCO we have performed full-potential LAPW band structure calculations. From an analysis of the density of states, the electric field gradient and the total energy we can rule out a tetravalent Pr, while our results are consistent with a Pr valency of 3+. The difference between the itinerant calculation and a simulation of Pr^{3+} is small, indicating that the band picture does not seriously overestimate the hybridization between Pr 4f states with copper and oxygen states. By the substitution of Y with Pr the charge at the plane atoms Cu(2), O(2) and O(3) is redistributed among different symmetries, leading to significantly changed EFGs and asymmetry parameters. Measurements of the EFG at the Pr site could probably clarify the valency of Pr.

Acknowledgments

The authors gratefully acknowledge the help of R Augustyn who speeded up the WIEN code used in the present work. The calculations were performed at the Computer Centre of the Technical University of Vienna on an S100 supercomputer (within the cooperation project with Siemens Nixdorf Informationssysteme) and partly at the Computing Centre of the University Graz. This project was supported by the Austrian 'Fonds zur Förderung der wissenschaftlichen Forschung', project number P8176.

References

[1] Tang X X, Manthiram A and Goodenough J B 1989 *Physica* C **161** 574
[2] Neumeier J J, Maple M B and Torikachvili M S 1988 *Physica* C **156** 574
[3] Hilscher G, Holland-Moritz E, Holubar T, Jostarndt H-D, Nekvasil V, Schaudy G, Walter U and Fillion G 1994 *Phys. Rev.* B submitted for publication
[4] Ambrosch-Draxl C, Blaha P and Schwarz K 1993 *Electronic Properties of High Temperature Superconductors and Related Compounds (Springer Series in Solid State Sciences 113)* p 430
[5] Guo G Y and Temmerman W M 1990 *Phys. Rev.* B **41** 6372
[6] Fehrenbacher R and Rice T M 1993 *Phys. Rev. Lett.* **70** 3471
[7] Neumeier J J, Bjornholm T, Maple M B, Rhyne J J and Gotaas J A 1990 *Physica* C **166** 191
[8] Blaha P, Schwarz K and Augustyn R 1993 *WIEN93* Technical University Vienna. Improved and updated version of the original copyrighted WIEN code, which was published by
Blaha P, Schwarz K, Sorantin P and Trickey S B 1990 *Comp. Phys. Commun.* **59** 399
[9] Kircher J, Cardona M, Gopalan S, Habermeier H-U and Fuchs D 1991 *Phys. Rev.* B **44** 2410
[10] Schwarz K, Ambrosch-Draxl C and Blaha P 1990 *Phys. Rev.* B 42 2051
[11] Fink J, Nücker N, Romberg H, Alexander M, Maple M B, Neumeier J J and Allen J W 1990 *Phys. Rev.* B 42 4823
[12] Blaha P, Schwarz K and Herzig P 1985 *Phys. Rev. Lett.* **54** 1192
[13] Ambrosch-Draxl C, Blaha P and Schwarz K 1991 *Phys. Rev.* B **44** 5141
[14] Reyes A P, MacLaughlin D E, Takigawa M, Hammel P C, Heffner R H, Thompson J D, Crow J E, Kebede A, Mihalisin T and Schwegler J 1990 *Phys. Rev.* B 42 2688